Charge-Density-Wave Phase Elasticity of the Blue Bronze

B. Hennion
Laboratoire Léon Brillouin, Centre d'Etudes de Saclay, 91191 Gif-sur-Yvette CEDEX, France

J. P. Pouget
Laboratoire de Physique des Solides, Bâtiment 510, Université Paris-Sud, 91405 Orsay CEDEX, France

M. Sato
Department of Physics, Nagoya University, Chikusa-ku, Nagoya 464-01, Japan
(Received 8 November 1991)

We report neutron inelastic scattering measurements of the dispersion of the phase mode of the charge-density-wave (CDW) collective excitations in the blue bronze. Anisotropy and temperature-dependence analysis yields phase elasticity parameters relevant for a classical deformable model of CDW. The considerable stiffening of the longitudinal phason velocity observed upon cooling clearly shows that Coulomb forces play a fundamental role in CDW deformation processes.

PACS numbers: 71.45.Lr, 63.20.Kr, 72.15.Nj

Quasi-1D conductors [1], such as $NbSe_3$, the blue bronze $K_{0.3}MoO_3$, and TTF-TCNQ, undergo a second-order Peierls transition which stabilizes a $2k_F$ incommensurate periodic lattice distortion whose dynamics correspond to the phase and amplitude oscillations of the charge density wave (CDW) [2]. As first recognized by Fröhlich [3] the phase of the CDW plays an especially important role because a rigid sliding of the $2k_F$ modulation carries in principle an electric current. Pinning by impurities and damping by normal carrier screening prevent Fröhlich superconductivity. However, the observation of a rich variety of nonlinear electronic transport phenomena has stimulated intense theoretical work in order to describe the CDW motion [1]. In the description proposed by Fukuyama, Lee, and Rice [4], the CDW ground state is considered as a classical anisotropic elastic medium, deformed by randomly distributed defects. CDW elasticity is due to the long-wavelength phase deformations. The first purpose of this Letter is to provide the corresponding elastic constants in the blue bronze $K_{0.3}MoO_3$, measured by inelastic neutron scattering.

In phase elasticity, intrachain deformations of the CDW imply a charge redistribution leading to long-range Coulomb forces, while interchain shear deformations only lead to phase shifts of adjacent CDW without charge redistribution [5]. At high temperatures the Coulomb forces are screened by the quasiparticles thermally excited through the Peierls gap, giving rise to an acousticlike phason dispersion in the chain direction [6], and to a damped CDW motion. At low temperature, when screening no longer exists, the longitudinal phason is opticlike [2,6] and the CDW becomes rigid. Evidence of Fröhlich sliding of a rigid CDW has been reported below 40 K in the blue bronze [1]. Our measurements have been performed in the temperature range where the longitudinal phason remains acoustic. However, they show a considerable stiffening of its velocity upon cooling which directly proves, and this is the second important aspect of this Letter, the drastic role of Coulomb forces in intrachain CDW deformation processes.

In Ref. [7] we have reported a neutron inelastic scattering study of the Peierls transition in $K_{0.3}MoO_3$, including the evolution of the Kohn anomaly above the Peierls transition ($T_c = 183$ K), the evolution of the amplitude mode below T_c, and an estimation of the longitudinal phason velocity (33 ± 5 THz Å at $T = 175$ K). Inspection of the phase mode did not allow an unambiguous observation of a gap, but a fit of the data at the incommensurate satellite position allowed the possibility of an overdamped phason gap with (at $T = 130$ K) $\omega_g = 0.2 \pm 0.1$ THz and $\Gamma = 0.8 \pm 0.2$ THz, where ω_g agrees with the frequency of the pinned collective mode obtained by millimeter-wave spectral-range measurements [8]. The present sample was the same as in Ref. [7] and the measurements have been carried out at the Laboratoire Léon Brillouin on the three-axis spectrometers 4F1 and 4F2 installed on a cold source of the Orphée reactor at Saclay. The main difficulties to overcome are related to the high velocity of the phase mode and to its damping. At low energy, $2k_F + q$ and $2k_F - q$ peaks, in a constant-energy measurement, cannot be separated and at higher energy, the proximity of the damped amplitude mode prevents clear-cut measurements.

Numerous measurements have been performed in various resolution conditions and in different scattering planes in order to cross-check as far as possible the extraction of physical parameters obtained from the data analysis. The main results concern the anisotropy of the phason velocity and its temperature dependence. In order to get information on the three main directions of anisotropy, $\mathbf{b}^*$ (along the chain direction), $2\mathbf{a}^* + \mathbf{c}^*$ (close to $2\mathbf{a} + \mathbf{c}$ perpendicular to the chain within the MoO_3 slabs), and $2\mathbf{a}^* - \mathbf{c}^*$ (perpendicular to the MoO_3 slabs), data have been collected near the incommensurate peaks (5,0.73,2.5) (scattering plane $\mathbf{b}^*, 2\mathbf{a}^* + \mathbf{c}^*$) and (−1, 3.27,0.5) (scattering plane $\mathbf{b}^*, 2\mathbf{a}^* - \mathbf{c}^*$). Examples of

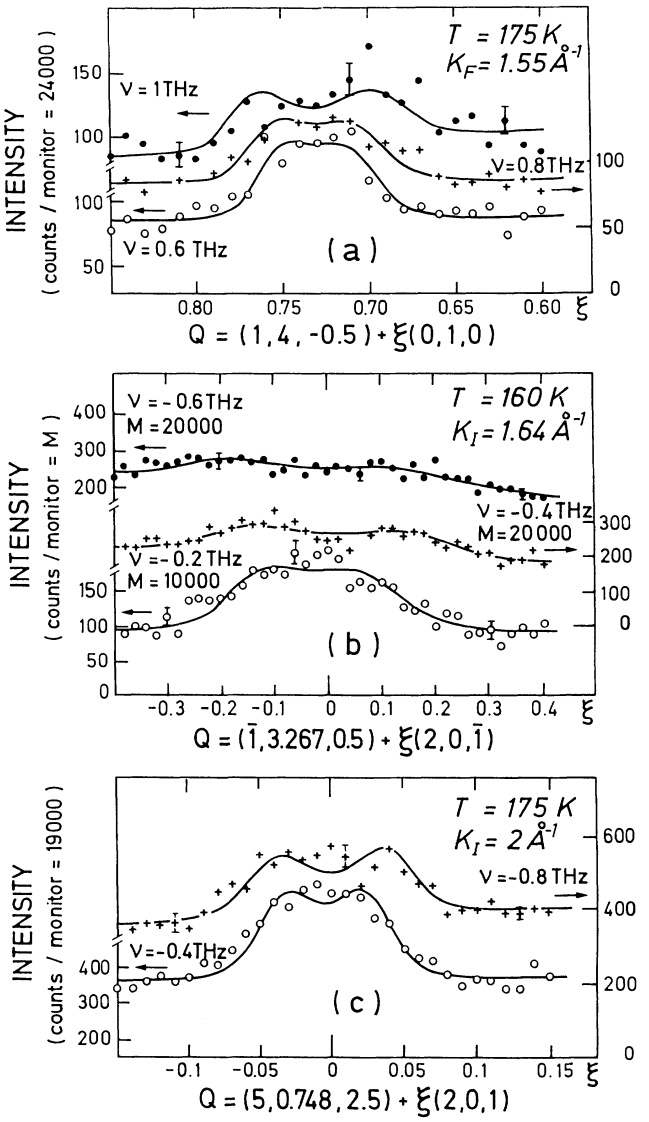

FIG. 1. Examples of ν scans through the phase mode along the (a) $\mathbf{b}^*$, (b) $2\mathbf{a}^*-\mathbf{c}^*$, and (c) $2\mathbf{a}^*+\mathbf{c}^*$ directions. Solid lines are fitted line shapes including damping.

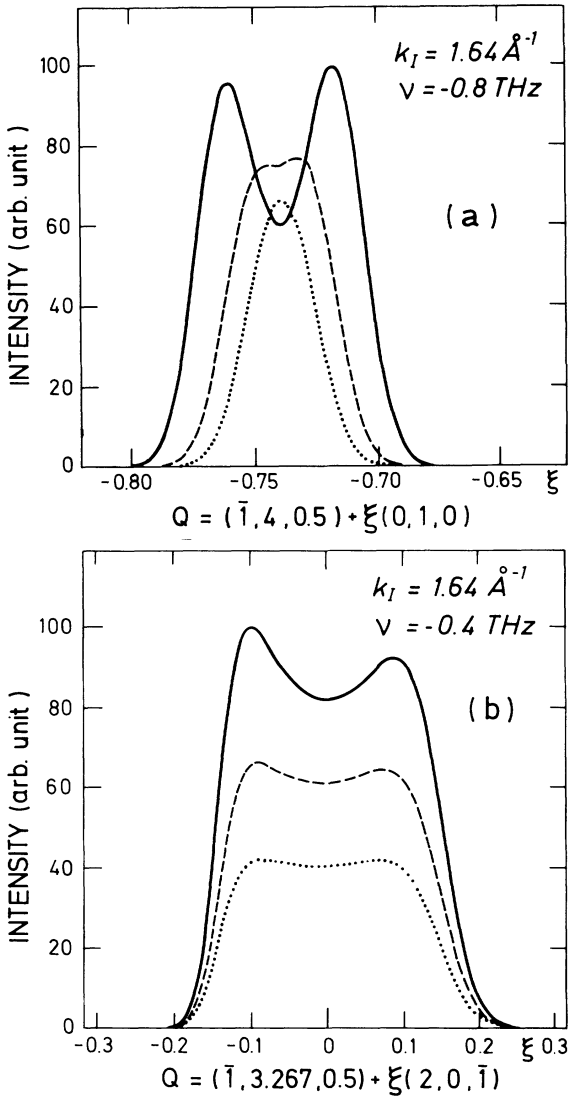

FIG. 2. Convolution of the resolution function with a dispersion surface $\omega^2=c_x^2q_x^2+c_y^2q_y^2+c_z^2q_z^2$, for the experimental conditions of the measurements reported in Fig. 3. z is perpendicular to the scattering plane. $c_y=3.6$ THz Å, $c_z=16$ THz Å, and $c_x=35$ (——), 60 (---), and 100 (· · ·) THz Å.

such measurements are displayed in Fig. 1.

Experimental results have been analyzed with the assumption of a damped harmonic oscillator, with an anisotropic dispersion: $\omega^2=c_x^2q_x^2+c_y^2q_y^2+c_z^2q_z^2$ $(+\omega_g^2)$, with x, y, and z corresponding to the $\mathbf{b}^*$, $2\mathbf{a}^*-\mathbf{c}^*$, and $2\mathbf{a}^*+\mathbf{c}^*$ directions. Figure 2 reports calculated profiles, accounting for experimental resolution, with no intrinsic linewidth, for realistic values of c_x, c_y, and c_z. Figure 2(a) demonstrates that in the b^* direction the Gaussian shape for the $\pm q$ peaks is preserved: Because of the large anisotropy a planar approximation of the dispersion is pertinent and the analysis will be little dependent on the velocity in other directions. Figure 2(b) emphasizes that the shape of the scattered intensity in the $2\mathbf{a}^*-\mathbf{c}^*$ direction is far from Gaussian and is strongly dependent on the velocity along b^*. Nevertheless the positions of the edges of the intensity contour yield a good estimation of the q values of the phonon in the transverse direction.

The final analysis has to account for the damping, which will essentially round the line shapes. It is obvious that the experimental difficulty described above will limit the accuracy of the determination of this parameter. Fortunately in a classical description of an incommensurate Peierls instability, the amplitude and phase modes have the same damping [9]. So we use the q dependence along b^* and the temperature dependence of the damping of the amplitude mode previously determined [7] to fix the damping of the phase mode. We have checked that

the determination of the velocities is not very sensitive to the precise value of the damping. At $T=175$ K, with a fixed damping value of 0.8 THz (FWHM), the phase-mode velocities $v_{b^*}=37\pm5$, $v_{2a^*+c^*}=16\pm3$, and $v_{2a^*-c^*}=3.6\pm0.6$ THzÅ are obtained. The solid lines in Fig. 1 are the profiles calculated with these values, including damping.

The large anisotropy of the phason velocity at 175 K, namely, 1:4.4(±1.6):10(±3) along the $2\mathbf{a}^*-\mathbf{c}^*$, $2\mathbf{a}^*+\mathbf{c}^*$, and $\mathbf{b}^*$ directions, respectively, is that expected from the anisotropy of other physical properties of the blue bronze, such as the electrical conductivity [10], the acoustic phonon velocities [7], or the lattice elastic constants [11]. More quantitatively, as expected from the quasiharmonic theory [12] of the incommensurate phase transition and as generally assumed in the phase elasticity Hamiltonian [1,4], the phason anisotropy near T_c agrees with that (1:3:10 [13]) of the correlation lengths involved in the CDW amplitude fluctuations above T_c. This anisotropy is fixed by the interchain CDW coupling energies [14]. In addition, the phason anisotropy is close to that of the CDW Lee-Rice domain lengths measured in 0.035 at.% irradiated 1:3.3:8.3 [15] or 2.4% V-doped 1:~3:~7 [16] blue bronzes.

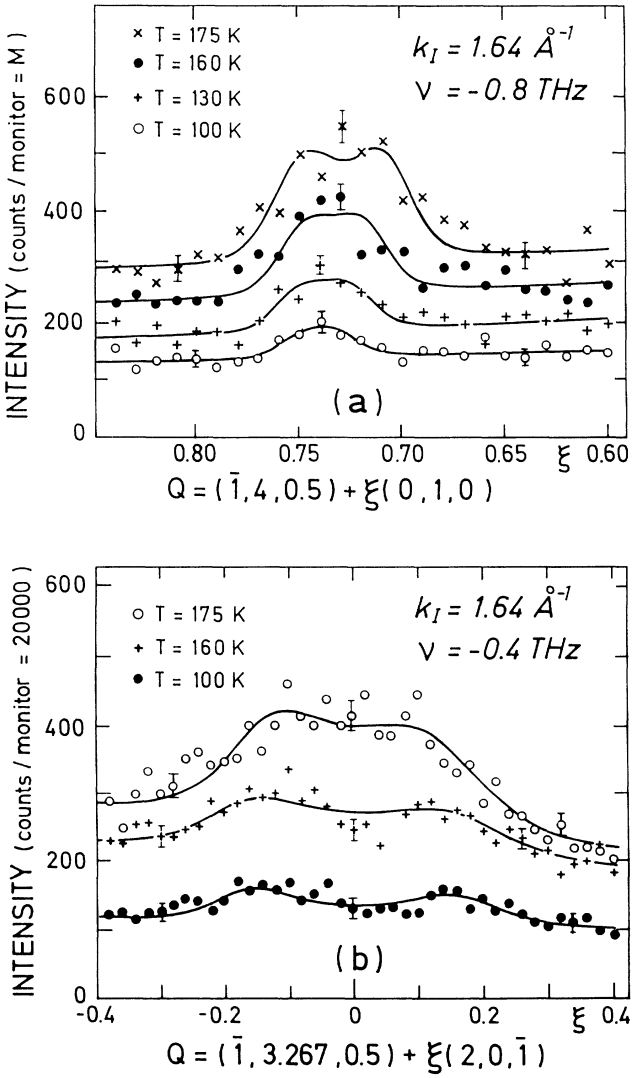

FIG. 3. ν scans through the phase mode along the (a) $\mathbf{b}^*$ and (b) $2\mathbf{a}^*-\mathbf{c}^*$ directions for various temperatures between 175 and 100 K. Solid lines are fitted line shapes. In (a) the data for $T\geq130$ K are measured with $M=20000$ (counting time ≃20 min) and reported for $M=30000$ (the monitor used at 100 K) (hence, error bars $=1.5\sqrt{\text{count}}$).

Phason velocity measurements were carried out down to 100 K and analyzed in the same way, using the temperature dependence of the amplitude mode damping. Figure 3 shows some of the constant-energy scans. We observe no significant variation of the velocity along $2\mathbf{a}^*-\mathbf{c}^*$. A similar observation is done along $2\mathbf{a}^*+\mathbf{c}^*$. This clearly proves that the shear deformation of the CDW sublattice does not imply significant charge redistribution. Such is not the case for the measurements performed along b^* where the scattered intensity is clearly seen to become q narrower upon cooling and centered on the position of the satellite reflection. The analysis of the $\nu=-0.8$ THz scans yields the temperature dependence of the phason velocity along b^* shown by open symbols in Fig. 4. Above T_c we have also reported the equivalent parameter for the Kohn anomaly, namely, c_K for $\omega^2=\omega_K^2+c_K^2(q-q_K)^2$, which outlines the continuity of excitations through the second-order Peierls transition. An attempt to go beyond the planar approximation, and to account for the anisotropy of the dispersion curves, still neglecting polarization effects, gives the solid symbols of Fig. 4.

In the temperature range studied, the longitudinal phason remains acousticlike. However, both sets of data shown in Fig. 4 give an enhancement of the longitudinal phason velocity by a factor of about 2.5 between 175 and

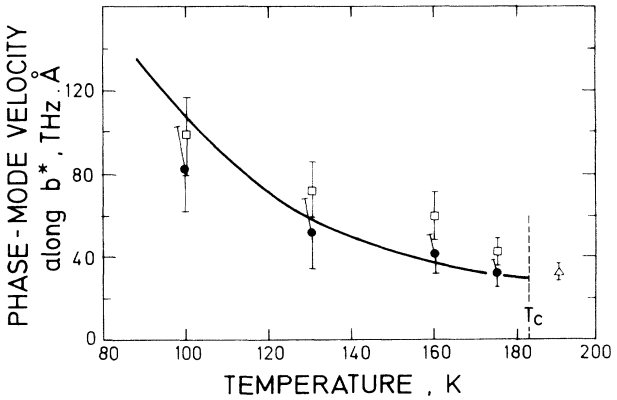

FIG. 4. Thermal evolution of the phase-mode velocity in the b^* direction neglecting (□) or accounting for (●) the anisotropy of the dispersion surface. The solid line is calculated from Eq. (1). △ is the curvature of the Kohn anomaly at 190 K.

100 K. Such a feature is observed neither in incommensurate dielectrics such as $ThBr_4$ nor on the transverse velocities in the blue bronze. It should therefore be ascribed to the thermal reduction of screening of the long-range Coulomb forces involved in phase deformations in the 1D direction. In the acoustic regime the phase-mode velocity renormalized by these effects is given by [6]

$$v_{b^*} = v_F \left(\frac{m_e}{m^*} \right)^{1/2} \left(1 + \frac{\exp(\Delta/T)}{(2\pi\Delta/T)^{1/2}} \right)^{1/2}, \quad (1)$$

where Δ is the temperature-dependent half Peierls gap, v_F is the Fermi velocity, and m^*/m_e is the CDW reduced mass [2].

Using, at $T=0$ K, $\Delta_0=565$ K [17] and the thermal dependence of Δ/Δ_0 from the variation of the square root of the satellite intensity [18], one obtains, after scaling with the 175-K data, the solid line displayed in Fig. 4. Within experimental accuracy, Eq. (1) satisfactorily accounts for the experimental increase of v_{b^*}. At 175 K Eq. (1) predicts that Coulomb forces have already stiffened the phason velocity by about 60%. With a Fermi velocity $v_F \sim 1.9\times10^5$ m/s [7] the longitudinal phason velocity measured at 175 K gives a CDW reduced mass m^*/m_e of 150, in good agreement with the value of 350 deduced from millimeter-wavelength-range conductivity measurements [8].

In conclusion, we have measured, for the first time in a low-dimensional conductor undergoing an incommensurate CDW ground state, the elasticity associated with the phase deformations of the collective mode, a key item of information for the CDW deformable models. We have also shown that the phase elasticity anisotropy can account for the shape of the Lee-Rice CDW domains measured in disordered blue bronzes. Finally our thermal measurements unambiguously prove that Coulomb forces are strongly involved in longitudinal CDW deformation processes.

This work has benefited from fruitful discussions with S. Barisic, C. Escribe-Filippini, and C. Schlenker. Laboratoire Léon Brillouin is associated with CEA and CNRS. Laboratoire de Physique des Solides is CNRS URA No. 2.

[1] For recent reviews, see *Low Dimensional Electronic Properties of Molybdenum Bronzes and Oxides,* edited by C. Schlenker (Klüwer Academic, Dordrecht, 1989); *Charge Density Waves in Solids,* Modern Problems in Condensed Matter Science Series Vol. 25, edited by L. P. Gork'ov and G. Gruner (Elsevier, New York, 1989).

[2] P. A. Lee, T. M. Rice, and P. W. Anderson, Solid State Commun. **14**, 703 (1974).

[3] H. Fröhlich, Proc. R. Soc. London A **223**, 296 (1954).

[4] H. Fukuyama and P. A. Lee, Phys. Rev. B **17**, 535 (1977); P. A. Lee and T. M. Rice, Phys. Rev. B **19**, 3970 (1979).

[5] See, for example, S. Barisic, in *Low Dimensional Conductors and Superconductors,* edited by D. Jérome and L. G. Caron, NATO Advanced Study Institutes, Ser. B, Vol. 155 (Plenum, New York, 1987), p. 395.

[6] Y. Nakane and S. Takada, J. Phys. Soc. Jpn. **54**, 977 (1985); K. Y. M. Wong and S. Takada, Phys. Rev. B **36**, 5476 (1987).

[7] J. P. Pouget, B. Hennion, C. Escribe-Filippini, and M. Sato, Phys. Rev. B **43**, 8421 (1991).

[8] T. W. Kim, D. Reagor, C. Gruner, K. Maxi, and A. Virosztek, Phys. Rev. B **40**, 5372 (1989).

[9] E. Tutis and S. Barisic, Phys. Rev. B **43**, 8431 (1991).

[10] J. P. Pouget, S. Kagoshima, C. Schlenker, and J. Marcus, J. Phys. (Paris), Lett. **44**, L113 (1983).

[11] L. C. Bourne and A. Zettl, Solid State Commun. **60**, 789 (1986); M. Saint-Paul and G. X. Tessema, Phys. Rev. B **39**, 8736 (1989).

[12] A. D. Bruce and R. A. Cowley, J. Phys. C **11**, 3609 (1978).

[13] S. Girault, A. H. Moudden, and J. P. Pouget, Phys. Rev. B **39**, 4430 (1989).

[14] J. P. Pouget, S. Girault, A. H. Moudden, B. Hennion, C. Escribe-Filippini, and M. Sato, Phys. Scr. **T25**, 58 (1989); J. P. Pouget, in *Low-Dimensional Electronic Properties of Molybdenum Bronzes and Oxides* (Ref. [1]), p. 87.

[15] S. M. Deland, G. Mozurkewich, and L. D. Chapman, Phys. Rev. Lett. **66**, 2026 (1991).

[16] These ratios have been obtained after having applied a Gaussian resolution correction to the data of S. Girault, A. M. Moudden, J. P. Pouget, and J. M. Godard, Phys. Rev. B **38**, 7980 (1988).

[17] D. C. Johnston, Phys. Rev. Lett. **52**, 2049 (1984).

[18] J. P. Pouget, C. Noguera, A. H. Moudden, and R. Moret, J. Phys. (Paris) **46**, 1731 (1985); **47**, 145(E) (1986). Also see earlier references therein.